Title
Rqc2p and 60S ribosomal subunits mediate mRNA-independent elongation of nascent chains

Journal
Science, 347(6217)

ISSN
0036-8075

Authors
Shen, Peter S
Park, Joseph
Qin, Yidan
et al.

Publication Date
2015-01-02

DOI
10.1126/science.1259724

Peer reviewed

HHS Public Access
Author manuscript
Science. Author manuscript; available in PMC 2015 June 02.

Published in final edited form as:
Science. 2015 January 2; 347(6217): 75–78. doi:10.1126/science.1259724.

Rqc2p and 60S ribosomal subunits mediate mRNA-independent elongation of nascent chains

Peter S. Shen[1], **Joseph Park**[2], **Yidan Qin**[8,9], **Xueming Li**[7,10], **Krishna Parsawar**[11], **Matthew H. Larson**[3,4,5,6], **James Cox**[1,11], **Yifan Cheng**[7], **Alan M. Lambowitz**[8,9], **Jonathan S. Weissman**[*,3,4,5,6], **Onn Brandman**[*,2], and **Adam Frost**[1,7,*]

[1]Department of Biochemistry, University of Utah, UT 84112, USA

[2]Department of Biochemistry, Stanford University, Palo Alto CA 94305, USA

[3]Department of Cellular & Molecular Pharmacology, University of California, San Francisco, San Francisco, CA 94158, USA

[4]Howard Hughes Medical Institute, University of California, San Francisco, San Francisco, CA 94158, USA

[5]California Institute for Quantitative Biomedical Research, University of California, San Francisco, San Francisco, CA 94158, USA

[6]Center for RNA Systems Biology, University of California, San Francisco, San Francisco, CA 94158, USA

[7]Department of Biochemistry and Biophysics, University of California, San Francisco, San Francisco, CA 94158, USA

[8]Institute for Cellular and Molecular Biology, University of Texas at Austin, Austin TX 78712, USA

[9]Department of Molecular Biosciences, University of Texas at Austin, Austin TX 78712, USA

[11]Mass Spectrometry and Proteomics Core Facility, University of Utah, UT 84112, USA

Abstract

In Eukarya, stalled translation induces 40S dissociation and recruitment of the Ribosome Quality control Complex (RQC) to the 60S subunit, which mediates nascent chain degradation. Here, we report cryoEM structures revealing that the RQC components Rqc2p (YPL009C/Tae2) and Ltn1p (YMR247C/Rkr1) bind to the 60S at sites exposed after 40S dissociation, placing the Ltn1p RING domain near the exit channel and Rqc2p over the P-site tRNA. We further demonstrate that Rqc2p

[*]To whom correspondence should be addressed: jonathan.weissman@ucsf.edu (J.S.W.), onn@stanford.edu (O.B.), adam.frost@ucsf.edu (A.F.).
[10]Present address: School of Life Sciences, Tsinghua University, Beijing 100084, China

Supplementary Materials
Materials and Methods
Figs. S1 to S13
Table S1
References (27–41)

The authors declare no competing financial interests.

The cryoEM structures have been deposited at the EMDB (accession codes 2811, 2812, 6169, 6170, 6171, 6172, and 6176).

recruits alanine and threonine charged tRNA to the A-site and directs elongation of nascent chains independently of mRNA or 40S subunits. Our work uncovers an unexpected mechanism of protein synthesis in which a protein—not an mRNA—determines tRNA recruitment and the tagging of nascent chains with Carboxy-terminal Ala and Thr extensions ("CAT tails").

Despite the processivity of protein synthesis, faulty messages or defective ribosomes can result in translational stalling and incomplete nascent chains. In Eukarya, this leads to recruitment of the RQC which mediates ubiquitylation and degradation of incompletely-synthesized nascent chains (1–4). The molecular components of the RQC include the AAA ATPase Cdc48p and its ubiquitin-binding cofactors, the RING-domain E3 ligase Ltn1p, and two proteins of unknown function, Rqc1p and Rqc2p. We set out to determine the mechanism(s) by which relatively rare (5) proteins like Ltn1p, Rqc1p, and Rqc2p recognize and rescue stalled 60S ribosome-nascent chain complexes, which are vastly outnumbered by ribosomes translating normally or in stages of assembly.

To reduce structural heterogeneity and enrich for complexes still occupied by stalled nascent chains, we immunoprecipitated Rqc1p-bound RQC assemblies from *S. cerevisiae* strains lacking the C-terminal RING domain of Ltn1p, which prevents substrate ubiquitylation and Cdc48 recruitment (1). 3D classification of Ltn1ΔRING particles revealed 60S ribosomes with nascent chains in the exit tunnel and extra-ribosomal densities (Fig 1). These extra-ribosomal features were resolved between 5Å and 14Å and proved to be either Tif6p or RQC components as characterized below (Figs 1, S1–7). Tif6p was not observed bound to the same 60S particles bound by RQC factors (Figs S1–3). We repeated the purification, imaging and 3D classification from *rqc2Δ* cells and computed difference maps. This analysis did not reveal density attributable to Rqc1p, but did identify Rqc2p as a tRNA-binding protein that occupies the 40S binding surface and Ltn1p as the elongated molecule that meets Rqc2p at the sarcin-ricin loop (SRL) (Figs 1–2, S1–S5). Comparison of the 60S-bound Ltn1p with reconstructions of isolated Ltn1p suggests that the N-terminus of Ltn1p engages the SRL with Rqc2p and that the middle region–which contains long HEAT/Armadillo repeats that adopt an elongated superhelical structure–reaches around the 60S (6). This conformation likely positions the C-terminal RING domain near the exit tunnel to ubiquitylate stalled nascent chains (Fig S5–6 and (7)).

A refined reconstruction of the Rqc2p-occupied class demonstrated that Rqc2p makes extensive contacts with an approximately P-site positioned (~P-site) tRNA (Figs 1–2, S7). Rqc2p has a long coiled-coil that makes direct contact with the SRL and the 60S P-stalk base (Fig 2A). This structure also revealed Rqc2p binding to an ~A-site tRNA whose 3′-CCA tail is within the peptidyl transferase center of the 60S (Fig 2B, S7). This observation was unexpected since A-site tRNA interactions with the large ribosomal subunit are typically unstable and require mRNA templates and elongation factors (8). Rqc2p's interactions with the ~A-site tRNA appeared to involve recognition between the anticodon loop and a globular N-terminal domain, as well as D-loop and T-loop interactions along Rqc2p's coiled coil (Figs 2–3).

To determine whether Rqc2p binds specific tRNA molecules, we extracted total RNA following RQC purification from strains with intact *RQC2* versus *rqc2Δ* strains. Deep sequencing by a new method (9) using a thermostable group II intron reverse transcriptase revealed that the presence of Rqc2p leads to a ~10-fold enrichment of $tRNA^{Ala(AGC)}$ and $tRNA^{Thr(AGT)}$ in the RQC (Fig 3A). In complexes isolated from strains with intact *RQC2*, Ala(AGC) and Thr(AGT) are the most abundant tRNA molecules, even though they are less abundant than a number of other tRNAs in yeast (10).

Our structure suggested that Rqc2p's specificity for these tRNAs is due in part to direct interactions between Rqc2p and positions 32-36 of the anticodon loop, some of which are edited in the mature tRNA (Fig 3). Adenosine 34 in the anticodon of both $tRNA^{Ala(AGC)}$ and $tRNA^{Thr(AGT)}$ is deaminated to inosine (11–13), leading to a diagnostic guanosine upon reverse transcription (13, 14) (Fig 3B–C). Further analysis of the sequencing data revealed that cytosine 32 in $tRNA^{Thr(AGT)}$ is also deaminated to uracil in ~70% of the Rqc2p-enriched reads (Fig 3 and (15)). Together with the structure, this suggests that Rqc2p binds to the D-, T- and anticodon loop of the ~A-site tRNA, and that recognition of the 32-UUIGY-36 edited motif accounts for Rqc2's specificity for these two tRNAs (Fig 3C–D). The pyrimidine at position 36 could explain the discrimination between the otherwise similar anticodon loops that harbor purines at base 36.

While assessing why Rqc2p evolved to bind these specific tRNA molecules, we considered these observations: first, our structural and biochemical data indicate that Rqc2p binds the 60S subunit *after* a stalled ribosome dissociates (Fig S6, *1, 2*). Second, stalled nascent chains accumulate as higher molecular weight species in the presence of Rqc2p than in its absence (Fig 4A, also seen in Fig 3E of (1)). Finally, amino acid addition to a nascent chain can be mediated by the large ribosomal subunit *in vitro* even when decoupled from a messenger RNA template and the small subunit (16). Together, these facts led us to hypothesize that Rqc2p may promote the extension of stalled nascent chains with alanine and threonine residues in an elongation reaction that is mRNA- and 40S-free. This hypothesis makes specific predictions. First, the Rqc2p-dependent increase in the molecular weight of the nascent chain should occur from the C-terminus exclusively. Second, the C-terminal extension should consist entirely of alanine and threonine residues that start immediately at the stalling sequence. Finally, the alanine and threonine extension should not have a defined sequence.

To test these predictions we expressed a series of reporters containing a stalling sequence (tracts of up to 12 consecutive arginine codons, including pairs of the difficult-to-decode CGA codon (17)), inserted between the coding regions of GFP and RFP (Fig 4A). Null mutations in RQC components or inhibition of the proteasome led to the accumulation of nascent chain fragments that are normally degraded in WT cells (Fig 4A) (1–4, 18). Furthermore, *ltn1*Δ and *rqc2*Δ cells have different phenotypes: expression of the stalling reporter in *ltn1*Δ led to formation and accumulation of higher molecular weight species that resolve as a smear ~1.5–5 kDa above the expected position of GFP (Fig 4A). GFP mass-shifted products are observable in *rqc1*Δ*ltn1*Δ double mutants, less prominent but still observable in *rqc1*Δ single mutants, but absent in all *rqc2*Δ single and double mutants (Fig 4A). Thus, Rqc2p is necessary for the production of these higher molecular weight GFP species.

We probed the location of the extra mass along the GFP by inserting a Tobacco Etch Virus (TEV) protease cleavage site upstream of the stalling tract (Fig 4B). GFP resolved as a single band of the expected size with TEV treatment, indicating that the extra mass is located at or after the stall sequence. To pinpoint the location of the extra mass along the GFP, we moved the TEV cleavage site after the R12 stalling sequence. This created a mass-shifted GFP that was insensitive to TEV treatment, suggesting that the post-R12 TEV cleavage site was not synthesized. One possible model is that a translational frame shift occurs near the R12 sequence which causes the mRNA to be mistranslated until the next out-of-frame stop codon. We falsified this model in two ways. First, we detected an Rqc2p-dependent GFP mass shift using a shorter R4 reporter in which multiple STOP codons were engineered in the +1 and +2 frames following the poly-arginine tract (Fig S8). Second, we detected the Rqc2p-dependent GFP mass shift in a construct encoding a hammerhead ribozyme. The ribozyme cleaves the coding sequence of the GFP mRNA, leaving a truncated non-stop mRNA that causes a stall during translation of its final codon (Fig S8, (19)). Thus the GFP mass shift is located at or after the stall sequence but cannot be explained by mRNA translation past the stalling tract in any frame.

In order to determine the composition of the GFP mass-shifted products, we performed total amino acid analysis of immunopurified GFP from strains expressing the stalling reporter. Purified GFP from *ltn1* (Fig 4C) or *rqc1* strains (Fig S9) is enriched in alanine and threonine compared to purified GFP from double mutants with *rqc2* which do not produce extended-GFP. We then used Edman degradation to sequence TEV release fragments following purification of the stalled GFP reporter from the *ltn1* strain. The first three codons in the R12 sequence are CGG-CGA-CGA, and Edman degradation suggested that the ribosome stalls at the first pair of the challenging-to-decode CGA codons (Fig S10). Following the encoded arginine residues, rising levels of alanine and threonine were detected at the C-terminus (Fig S10). We further characterized these fragments by mass spectrometry and detected diverse poly-Ala and poly-Thr species ranging from 5 to 19 residues with no defined sequence (Table S1). Together, these observations demonstrate that Rqc2p directs the elongation of stalled nascent chains with non-templated Carboxy-terminal Ala and Thr extensions or “CAT tails”.

Earlier work (1) revealed that accumulation of stalled nascent chains (e.g., by deletion of *LTN1*) led to a robust heat shock response that is fully dependent on Rqc2p, although the mechanism by which Rqc2p enabled this stress response was unclear. Here, we hypothesized that CAT tails may be required for activation of Heat Shock Factor 1 (Hsf1p). To isolate the effect of CAT tails in this context, we sought an *rqc2* allele that could not support CAT tails synthesis but could still bind to the 60S and facilitate Ltn1p-dependent ubiquitylation of the nascent chains. Rqc2p belongs to the conserved NFACT family of nucleic acid-binding proteins (20) and the N-terminal NFACT-N domain of Rqc2p is 22% identical to the NFACT-N domain of the *S. aureus* protein Fbp (PDB:3DOA). Based on sequence and predicted secondary structure conservation, we fit this structure into a portion of the cryoEM density ascribed to Rqc2p (Figs S11–12). This modeling exercise predicts that Rqc2p’s NFACT-N domain recognizes features of both the P- and A-site tRNA molecules and that conserved residues, D9, D98 and R99—which have been hypothesized to play roles in nucleic-acid binding or modifying reactions (20)—may contact the ~A-site tRNA (20) (Fig S12). An Rqc2p variant in which these residues were mutated to alanine (*rqc2$_{aaa}$*) rescued 60S recognition and the clearance of the stalling reporter almost as effectively as wild type Rqc2p, but did not support CAT tail synthesis (Figs 4D, S12). This CAT tail-deficient *rqc2$_{aaa}$* allele also failed to rescue Hsf1p transcriptional activation (Fig 4E), indicating that CAT tails may promote Hsf1p activation.

Integrating our observations, we propose the model schematized in Fig S13. Ribosome stalling leads to dissociation of the 60S and 40S subunits, followed by recognition of the peptidyl-tRNA-60S species by Rqc2p and Ltn1p. Ltn1p ubiquitylates the stalled nascent chain, and this leads to Cdc48 recruitment for extraction and degradation of the incomplete translation product. Rqc2p, through specific binding to Ala(IGC) and Thr(IGU) tRNAs, directs the template-free and 40S-free elongation of the incomplete translation product with CAT tails. CAT tails induce a heat shock response through a mechanism that is yet to be determined.

Hypomorphic mutations in the mammalian homolog of *LTN1* cause neurodegeneration in mice (21). Similarly, mice with mutations in a CNS-specific isoform of tRNA^{Arg} and GTPBP2, a homolog of yeast Hbs1 which works with PELOTA/Dom34 to dissociate stalled 80S ribosomes, suffer from neurodegeneration (22). These observations speak to the consequences that ribosome stalls impose on the cellular economy. Eubacteria rescue stalled ribosomes with the tmRNA-SmpB system, which appends nascent chains with a unique C-terminal tag that targets the incomplete protein product for proteolysis (23). The mechanisms utilized by eukaryotes, which lack tmRNA, to recognize and rescue stalled ribosomes and their incomplete translation products have been unclear. The RQC—and Rqc2p's CAT tail tagging mechanism in particular—bear both similarities and contrasts to the tmRNA *trans*-translation system. The evolutionary convergence upon distinct mechanisms for extending incomplete nascent chains at C-terminus argues for their importance in maintaining proteostasis. One advantage of tagging stalled chains is that it may distinguish them from normal translation products and facilitate their removal from the protein pool. An alternate, not mutually exclusive, possibility is that the extension serves to test the functional integrity of large ribosomal subunits so that the cell can detect and dispose of defective large subunits that induce stalling.

Supplementary Material

Refer to Web version on PubMed Central for supplementary material.

Acknowledgments

Electron microscopy was performed at the University of Utah and the University of California. We thank David Belnap (Utah) and Michael Braunfeld (UCSF) for supervision of the electron microscopes. We thank Anita Orendt and the Utah Center for High Performance Computing and the NSF XSEDE consortium for computational support. We thank David Sidote (UT Austin) for help processing RNA-seq data. We thank Daniel Herschlag and Pehr Harbury for helpful comments. Amino acid analysis was performed by John Shulze at the UC Davis Proteomics Core. Edman sequencing was performed at Stanford's Protein and Nucleic Acid Facility by Dick Winant. This work was supported by the Searle Scholars Program (A.F.), Stanford University (O.B.), NIH grants 1DP2GM110772-01 (A.F.), GM37949 and GM37951 (A.M.L.), the Center for RNA Systems Biology P50 GM102706 (J.S.W.) and U01 GM098254 (J.S.W.) and the Howard Hughes Medical Institute (J.S.W.).

References and Notes

1. Brandman O, et al. A ribosome-bound quality control complex triggers degradation of nascent peptides and signals translation stress. Cell. 2012; 151:1042–54. [PubMed: 23178123]
2. Defenouillère Q, et al. Cdc48-associated complex bound to 60S particles is required for the clearance of aberrant translation products. Proc Natl Acad Sci U S A. 2013:1221724110.
3. Verma R, Oania RS, Kolawa NJ, Deshaies RJ. Cdc48/p97 promotes degradation of aberrant nascent polypeptides bound to the ribosome. Elife. 2013; 2:e00308. [PubMed: 23358411]
4. Shao S, Von der Malsburg K, Hegde RS. Listerin-dependent nascent protein ubiquitination relies on ribosome subunit dissociation. Mol Cell. 2013; 50:637–648. [PubMed: 23685075]
5. Li GW, Burkhardt D, Gross C, Weissman JS. Quantifying Absolute Protein Synthesis Rates Reveals Principles Underlying Allocation of Cellular Resources. Cell. 2014; 157:624–635. [PubMed: 24766808]
6. Lyumkis D, et al. Single-particle EM reveals extensive conformational variability of the Ltn1 E3 ligase. Proc Natl Acad Sci U S A. 2013; 110:1702–7. [PubMed: 23319619]
7. Shao S, Hegde RS. Reconstitution of a Minimal Ribosome-Associated Ubiquitination Pathway with Purified Factors. Mol Cell. 201410.1016/j.molcel.2014.07.006
8. Lill R, Robertson JM, Wintermeyer W. Affinities of tRNA binding sites of ribosomes from Escherichia coli. Biochemistry. 1986; 25:3245–3255. [PubMed: 3524675]
9. Katibah GE, Qin Y, Sidote DJ, Yao J, Lambowitz AM, Collins K. Broad and adaptable RNA structure recognition by the human interferon-induced tetratricopeptide repeat protein IFIT5. Proc Natl Acad Sci USA. 2014; 111:12025–30. [PubMed: 25092312]
10. Chu D, Barnes DJ, von der Haar T. The role of tRNA and ribosome competition in coupling the expression of different mRNAs in Saccharomyces cerevisiae. Nucleic Acids Res. 2011; 39:6705–14. [PubMed: 21558172]
11. Agris PF, Vendeix FAP, Graham WD. tRNA's wobble decoding of the genome: 40 years of modification. J Mol Biol. 2007; 366:1–13. [PubMed: 17187822]
12. Crick FHC. Codon—anticodon pairing: The wobble hypothesis. J Mol Biol. 1966; 19:548–555. [PubMed: 5969078]
13. Gerber AP, Keller W. An adenosine deaminase that generates inosine at the wobble position of tRNAs. Science. 1999; 286:1146–1149. [PubMed: 10550050]
14. Delannoy E, et al. Arabidopsis tRNA adenosine deaminase arginine edits the wobble nucleotide of chloroplast tRNAArg(ACG) and is essential for efficient chloroplast translation. Plant Cell. 2009; 21:2058–71. [PubMed: 19602623]
15. Rubio MAT, Ragone FL, Gaston KW, Ibba M, Alfonzo JD. C to U editing stimulates A to I editing in the anticodon loop of a cytoplasmic threonyl tRNA in Trypanosoma brucei. J Biol Chem. 2006; 281:115–20. [PubMed: 16269406]
16. Monro RE. Protein Synthesis: Uncoupling of Polymerization from Template Control. Nature. 1969; 223:903–905. [PubMed: 4896042]
17. Letzring DP, Dean KM, Grayhack EJ. Control of translation efficiency in yeast by codon-anticodon interactions. RNA. 2010; 16:2516–28. [PubMed: 20971810]
18. Ito-Harashima S, Kuroha K, Tatematsu T, Inada T. Translation of the poly(A) tail plays crucial roles in nonstop mRNA surveillance via translation repression and protein destabilization by proteasome in yeast. Genes Dev. 2007; 21:519–524. [PubMed: 17344413]
19. Kobayashi K, et al. Structural basis for mRNA surveillance by archaeal Pelota and GTP-bound EF1α complex. Proc Natl Acad Sci U S A. 2010; 107:17575–17579. [PubMed: 20876129]
20. Burroughs AM, Aravind L. A highly conserved family of domains related to the DNA-glycosylase fold helps predict multiple novel pathways for RNA modifications. RNA Biol. 2014; 11:360–72. [PubMed: 24646681]
21. Chu J, et al. A mouse forward genetics screen identifies LISTERIN as an E3 ubiquitin ligase involved in neurodegeneration. Proc Natl Acad Sci U S A. 2009; 106:2097–103. [PubMed: 19196968]

22. Ishimura R, et al. Ribosome stalling induced by mutation of a CNS-specific tRNA causes neurodegeneration. Science (80-). 2014; 345:455–459.
23. Moore SD, Sauer RT. The tmRNA system for translational surveillance and ribosome rescue. Annu Rev Biochem. 2007; 76:101–124. [PubMed: 17291191]
24. Gerber A, Grosjean H, Melcher T, Keller W. Tad1p, a yeast tRNA-specific adenosine deaminase, is related to the mammalian pre-mRNA editing enzymes ADAR1 and ADAR2. EMBO J. 1998; 17:4780–4789. [PubMed: 9707437]
25. Gaston KW, et al. C to U editing at position 32 of the anticodon loop precedes tRNA 5′ leader removal in trypanosomatids. Nucleic Acids Res. 2007; 35:6740–9. [PubMed: 17916576]
26. Crooks GE, Hon G, Chandonia JM, Brenner SE. WebLogo: A sequence logo generator. Genome Res. 2004; 14:1188–1190. [PubMed: 15173120]

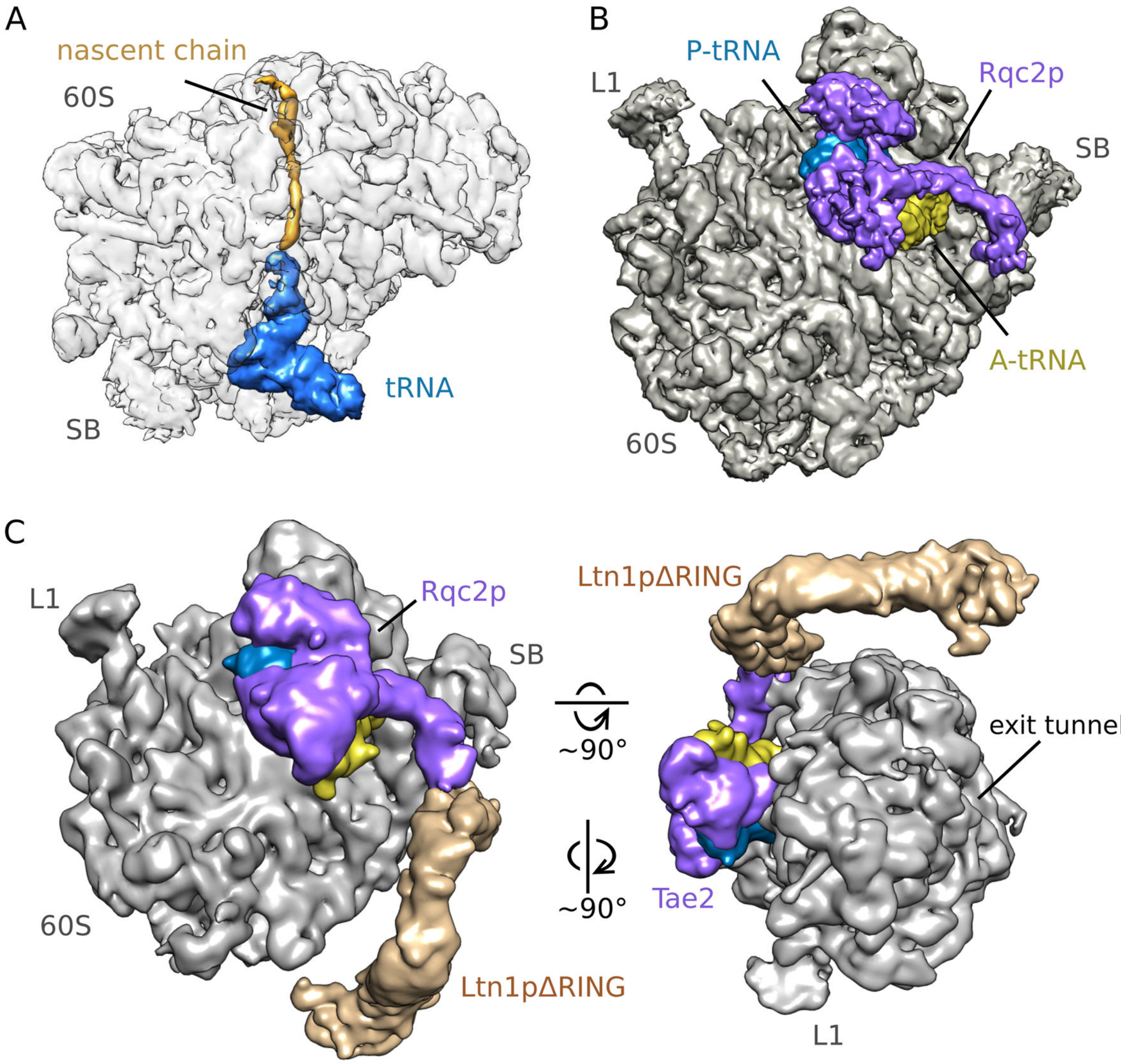

Figure 1. CryoEM reconstructions of peptidyl-tRNA-60S ribosomes bound by the RQC components Rqc2p and Ltn1p

A) A peptidyl-tRNA-60S complex isolated by immunoprecipitation of Rqc1p. The ribosome density is transparent to visualize the nascent chain. **B)** Rqc2p (purple) and an ~A-site tRNA (yellow) bound to peptidyl-tRNA-60S complexes. Landmarks indicated (L1, L1 stalk; SB, P-stalk base). **C)** Ltn1p (tan) bound to Rqc2p-peptidyl-tRNA-60S complexes (B).

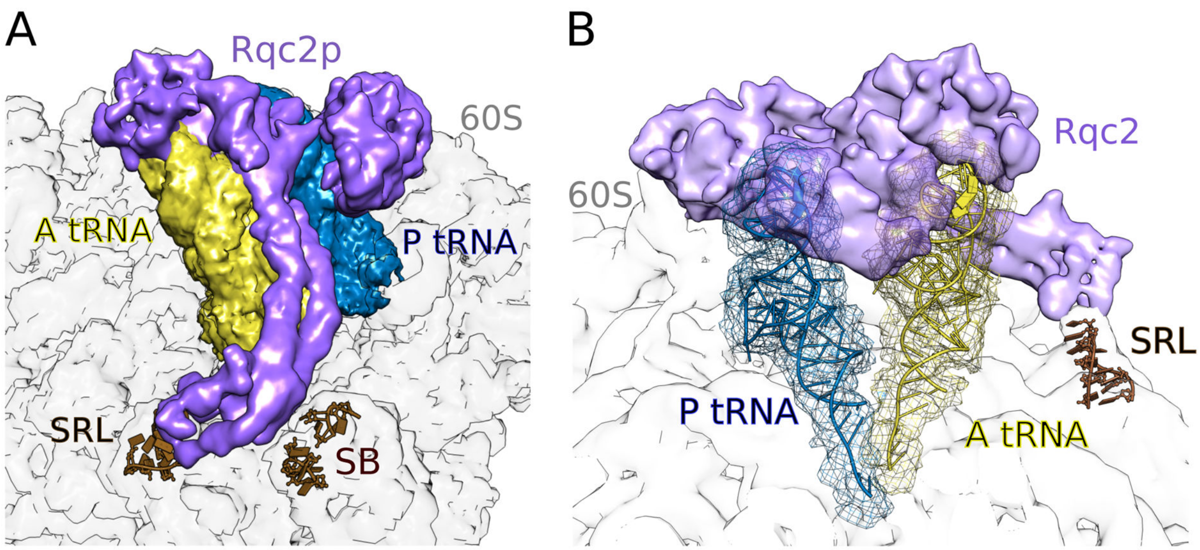

Figure 2. Rqc2p binding to the 60S ribosome, ~P-site and ~A-site tRNAs

A) Rqc2p contacts ~P- and ~A-site tRNAs, the sarcin-ricin loop (SRL) and P-stalk base rRNA (SB). **B)** Rigid body fitting of tRNAs structures (ribbons) into EM densities (mesh).

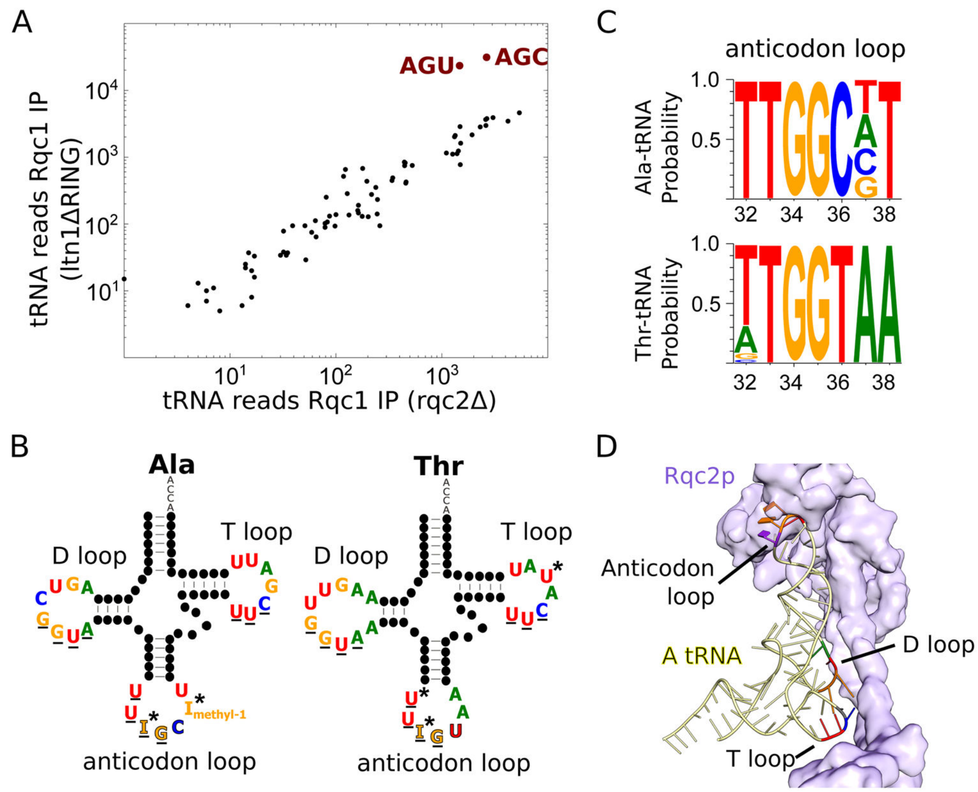

Figure 3. Rqc2p-dependent enrichment of tRNA$^{Ala(IGC)}$ and tRNA$^{Thr(IGU)}$

A) tRNA cDNA reads extracted from purified RQC particles and summed per unique anticodon, with versus without Rqc2p. **B)** Secondary structures of tRNA$^{Ala(IGC)}$ and tRNA$^{Thr(IGU)}$. Identical nucleotides underlined. Edited nucleotides indicated with asterisks (24, 25). **C)** Weblogo representation of cDNA sequencing reads related to shared sequences found in anticodon loops (positions 32-38) of mature tRNA$^{Ala(IGC)}$ and tRNA$^{Thr(IGU)}$(26). **D)** ~A-tRNA contacts with Rqc2p at the D-, T-, and anticodon loops. Identical nucleotides between tRNA$^{Ala(IGC)}$ and tRNA$^{Thr(IGU)}$ colored as in panel B (A, green; U, red; C, blue; G, orange) and pyrimidine, purple. Anticodon nucleotides are indicated as slabs.

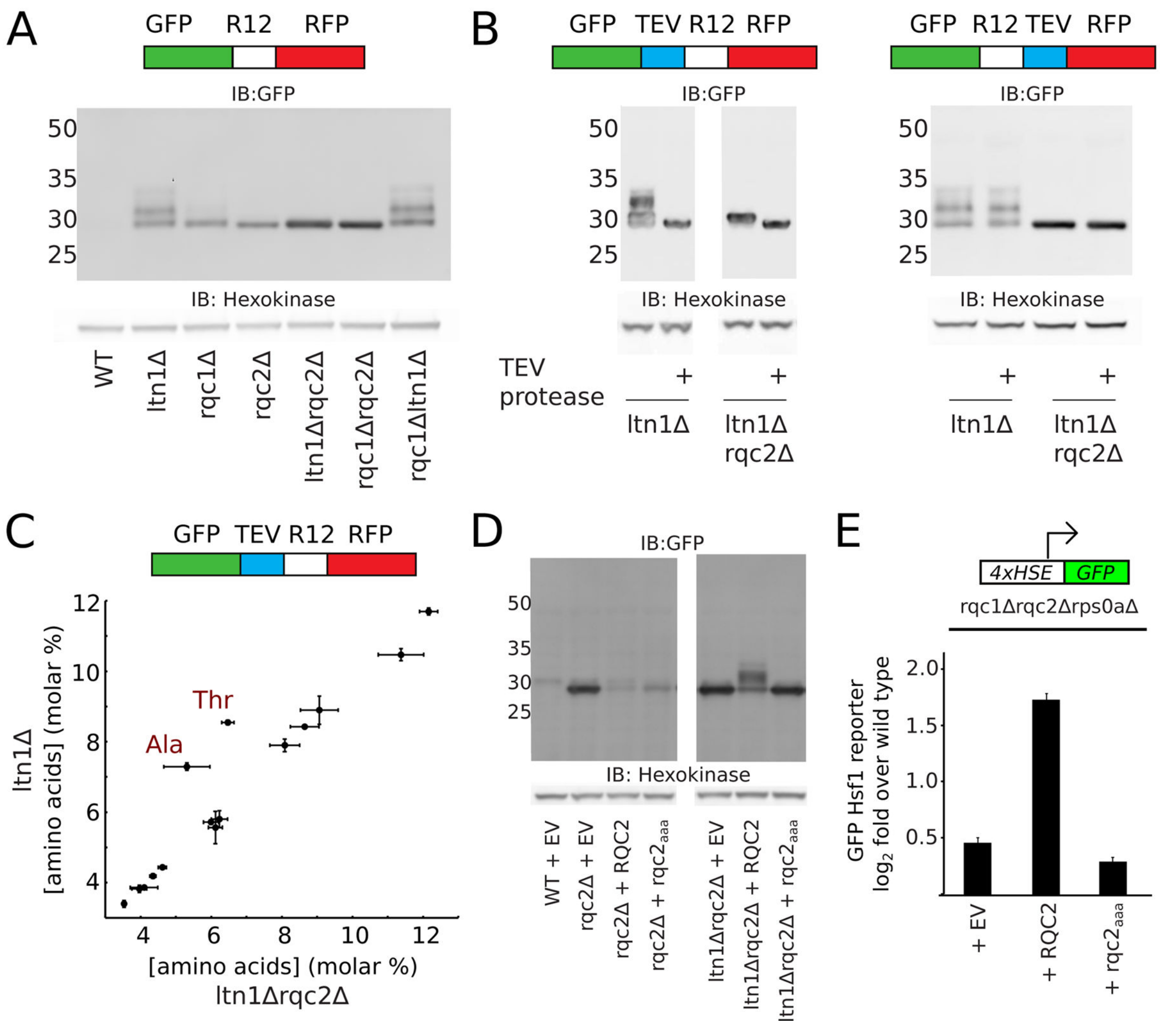

Figure 4. Rqc2p-dependent formation of CAT tails

A–B, D) Immunoblots of stalling reporters in RQC deletion strains. **C)** Total amino acid analysis of immunoprecipitated GFP expressed in *ltn1*Δ and *ltn1*Δ*rqc2*Δ strains, N=3. **E)** Triplicate GFP levels measured with a flow cytometer and normalized to a wild type control. EV=empty vector. All error bars are standard deviations.